5-2011

Calcium Provision in a Placentotrophic Lizard: Structural Differentiation Reflects Functional Specialization.

Haley K. Stinnett
East Tennessee State University

CALCIUM PROVISION IN A PLACENTOTROPHIC LIZARD:

STRUCTURAL DIFFERENTIATION REFLECTS FUNCTIONAL SPECIALIZATION

Thesis submitted in partial fulfillment of Honors

By

Haley Katherine Stinnett
The Honors College
University Honors Program
East Tennessee State University

April 2011

Dr. James R. Stewart, Faculty Mentor

Dr. Tom W. Ecay, Faculty Reader

Dr. Rebecca A. Pyles, Faculty Reader

ABSTRACT

Viviparity (live birth) and placentation have evolved in more than 100 lineages of squamate reptiles. However, highly placentotrophic species in which embryos receive the majority of nutrients for development via maternal transport across a placenta are rare. *Pseudemoia pagenstecheri* is a viviparous Australian scincid lizard with extensive placental transfer of nutrients. For example, 90% of neonate calcium is received via placental transfer. This species has a regionally differentiated chorioallantoic placenta distinguished by an elliptical-shaped region, the placentome. The placentome is characterized by hypertrophied uterine and embryonic epithelial cells supported by dense vascular networks. The remainder of the chorioallantoic placenta is also highly vascularized but epithelia are thin. A yolk sac placenta with hypertrophied epithelia is located in the abembryonic hemisphere of the egg. We used immunohistochemistry and immunoblotting to test the hypothesis that the placenta has regional functional specializations for calcium transport. Calcium uptake by extraembryonic membranes of squamates is correlated with expression of the intracellular calcium binding protein, calbindin-D_{28K}. Immunohistochemistry was used to localize calbindin-D_{28K} expressing cells. Immunoblotting for calbindin-D_{28K} and the plasma membrane calcium ATPase (PMCA, an additional marker for active calcium transport) was used to assess changes in protein expression levels through development. We found support for our hypothesis because calbindin-D_{28K} was expressed in the embryonic epithelium of the yolk sac placenta and in the chorionic epithelium of the placentome, but not in the remainder of the chorioallantoic placenta. In addition, calbindin-D_{28K} was expressed the chorioallantoic membrane in all embryonic stages studied, which encompassed both early and late development. Immunoblotting data show that calbindin-D_{28K} expression was detectable at low levels in early stages of development and increased

significantly prior to birth, when embryonic calcium demand peaks. Expression of PMCA also increases significantly throughout development, though less dramatically. Expression of calbindin-D_{28K} and PMCA protein by the chorioallantoic placenta parallels the accrual of calcium in the embryo. These data suggest that placental calcium secretion occurs over an extended interval of gestation, with increasing activity as embryonic demand escalates in late development. In conclusion, our results support our original hypothesis that regional structural differentiation in the placenta reflects functional specializations for calcium transport to the embryo during development.

INTRODUCTION

The transition from egg-laying (oviparity) to live-bearing (viviparity) has occurred on multiple occasions within the order Squamata (lizards and snakes) (Blackburn 1982, 1985, 1992, 2006; Shine, 1985). Most viviparous species are predominantly lecithotrophic, i.e., yolk provides most of the nutrients for embryonic development. Predominantly lecithotrophic species may also receive nutrients from placental transport, but the evolution of substantial placentotrophy is relatively rare. Embryos of predominantly placentotrophic species receive the majority of nutrients needed for development via maternal provision across a placenta. In a fully placentotrophic species, the placenta would fulfill all the nutritive, respiratory and excretory needs of the developing embryo (Stewart and Thompson, 2009). Of the 100+ clades of viviparous squamates, substantial placentotrophy has only been documented in four or five lineages of scincid lizards (Blackburn and Flemming, 2009). Placentae of females in each of these lineages contain structural elaborations that are thought to be specializations for transport (Weekes 1935; Blackburn, 1992, 1993; Stewart and Thompson, 1996; Blackburn and Flemming, 2009). However, our understanding of the function of specific placental structures is limited.

The genus *Pseudemoia* is a monophyletic lineage consisting of six species (Smith, 2001), three of which, *P. entrecasteauxii*, *P. pagenstecheri* and *P. spenceri*, have been studied extensively. These species share similar structural elaborations of both the chorioallantoic and yolk sac placentae and all are substantially placentotrophic (Stewart and Thompson, 1993, 1996, 1998, 2000; Thompson et al., 1999[a,b]). The chorioallantoic placenta contains two regions, placentome and paraplacentome, with different structural characteristics that likely support different functions. The terminal yolk sac placentation is an omphaloplacenta. Placental ontogeny is known for *P. entrecasteauxii* (Stewart and Thompson, 1996) and *P. spenceri*

(Stewart and Thompson, 1998) but only the terminal placental stage has been described for *P. pagenstecheri*. (Stewart and Thompson, 1996). Placental transport of calcium is substantial in all three species; for *P. pagenstecheri*, 90% of neonatal calcium is acquired via maternal provision across the placenta (Thompson et al., 1999[b]). Transcellular calcium transport is correlated with expression of calbindin-D_{28K} , a cytosolic calcium-binding protein, and expression of plasma membrane Ca^{2+} ATPase, a membrane-bound calcium exporter, in a variety of tissues (Feher et al., 1992; Bindels, 1993), including the chorioallantoic membrane of an oviparous snake, *Elaphe guttata* (Ecay et al., 2004).

We studied a developmental series of *Pseudemoia pagenstecheri* to describe placental ontogeny and used immunohistochemistry to localize calbindin-D_{28K} in placental tissues from this embryological series to test the hypothesis that structural elaborations in the chorioallantoic and yolk sac placentae serve functionally specialized roles in calcium transport. We also used immunoblotting techniques to estimate expression of calbindin-D_{28K} and plasma membrane Ca^{2+} ATPase in chorioallantoic membrane of siblings of these embryos and compared these data to prior research on embryonic uptake of calcium in *P. pagenstecheri* to test the hypothesis that expression of calcium transport proteins in chorioallantoic membrane is correlated with embryonic uptake of calcium from the placenta.

MATERIALS AND METHODS

Specimens used in this experiment are siblings of embryos that contributed to a study of the pattern of embryonic calcium mobilization (Stewart et al., 2009[a]). Female *Pseudemoia pagenstecheri* (n=24) were collected from field sites in New South Wales, transported to The University of Sydney, and maintained in a controlled environmental room (20°C, 12/12 photophase/scotophase). Females were housed in glass aquaria in groups of five or six individuals. Each aquaria was supplied with a 25 W incandescent bulb, which provided 12 h of elevated temperature daily. All animals were given rocks for basking, water, and fed twice weekly with mealworms (*Tenebrio molitor*) and crickets (*Acheta domesticus*) dusted with multivitamins and phosphorus-free calcium (Herpevite Rep-Cal CA, USA).

Females were killed by an overdose of sodium pentobarbital at various stages of gestation. Uterine incubation chambers, containing embryos, were surgically removed and processed in one of two protocols. For immunohistochemistry, the intact incubation chamber was fixed in 10% neutral buffered formalin for 15 minutes at which time the embryo was dissected free. The remaining tissues (uterus, chorioallantoic membrane, yolk sac) were left intact, fixed overnight in 10% neutral buffered formalin, washed in distilled water and stored in 70% ethanol. For immunoblots, embryos were dissected free of the uterus and the uterus, chorioallantoic membrane and yolk sac were each placed in mammalian cell lysis buffer (Sigma) at a wet mass: volume ratio of 1:5 (gr/ml) and frozen in liquid nitrogen. All embryos were fixed in 10% neutral buffered formalin and retained for staging, based on the system of Dufaure and Hubert (1961).

Immunohistochemistry: Following dehydration and clearing, the tissues were embedded in paraffin, sectioned at 7 μm, and mounted on slides for processing. Structural descriptions were obtained by observation of specimens stained with hematoxylin and eosin. Calbindin-D_{28K} was localized by immunohistochemical methods using a commercially available monoclonal antibody (Table 1). Tissue sections were deparaffinized, hydrated and treated with 0.3% hydrogen peroxide/methanol to eliminate endogenous peroxidase activity. Sections were then rinsed with phosphate buffered saline (PBS) and treated with 0.5% Triton X-100 in PBS to guard against non-specific binding. After three more washes with PBS, 5% normal goat serum in PBS was used as a blocking solution. Experimental specimens were treated with primary antibody (one hour) diluted in 5% horse serum/PBS. Control specimens were treated with 5% horse serum /PBS (one hour). After a series of washes with PBS, all specimens were incubated with secondary antibody, treated with peroxidase-conjugated streptavidin and washed again with PBS. All tissue was treated with diaminobenzidine tetrahydrochloride (DAB) and rinsed in water. Hematoxylin was used as a counterstain. The sections were dehydrated and cover-slipped using Cytoseal mounting medium.

Immunoblots: Cell lysis buffer (1:1 quantity) was added to each sample prior to homogenization. Tissues were homogenized in centrifuge tubes using 1 mm glass beads in a tissue vortex. Homogenization was achieved by vortexing at 4° C. Duplicate 25 μL aliquots were prepared for protein determination (BCA assay; Pierce). Tissue samples were diluted in electrophoresis sample buffer and proteins separated by sodium dodecyl sulfate-polyacrylamide gel electrophoresis (SDS-PAGE; Laemmli, 1970). Proteins were electrophoretically transferred (Towbin et al., 1979) to PDVF membranes (Millipore). For calbindin-D_{28K} immunodetection, rabbit polyclonal against recombinant corn snake calbindin-D_{28K} primary antibody (1:10,000

dilution; Ecay and Stewart, unpublished) and peroxidase-conjugated donkey anti-rabbit IgG secondary antibody (1:200,000 dilution; GE Healthcare) were used. For plasma membrane Ca^{2+} ATPase (PMCA) immunodetection, mouse monoclonal (clone 5F10) against human PMCA primary antibody (1:2000 dilution; Sigma) and peroxidase-conjugated sheep anti-mouse IgG secondary antibody (1:20000 dilution; GE Healthcare) were used. Actin immunoblotting was used as an internal standard for sample preparation and gel protein loading. Mouse monoclonal (clone C4) against chicken gizzard actin primary antibody (1:50,000; Millipore) and peroxidase-conjugated sheep anti-mouse IgG secondary antibody (1:200,000 dilution; GE Healthcare) were used in the immunodetection of actin (Table 1).

For immunodetection, PVDF blots were incubated in blocking buffer (5% nonfat dry milk, 2% horse serum, 0.05% Tween-20, 0.05% sodium azide in Tris-buffered saline (TBS; pH 7.4)) for one hour at room temperature. Blots were then incubated in primary antibody in blocking buffer at 4°C overnight. Primary antibodies were removed with three washes of blocking buffer, followed by three washes of blocking buffer without sodium azide. Blots were incubated for 2 hours at room temperature in blocking buffer (without sodium azide) that contained peroxidase-conjugated secondary antibody. After extensive washing in TBS, immune complexes were visualized on x-ray film by chemiluminescence using Immobilon Western reagent (Millipore). After immunodetection, blots were washed twice in TBS and cleared of adherent antibodies with two washes in stripping buffer (0.05M glycine HCl (pH 2.5-3.0), 0.02% SDS, 0.1% Tween-20 in dH_20). Blots were washed twice in TBS and stored dry for later reprobing. Immunoblot results were quantified by scanning densitometry using a flatbed scanner (Epson V500) and UN-SCAN-IT Gel™ 5.3 digitizing software (Silk Scientific).

Each individual blot (n = 10) included samples from the range of developmental stages (31-40). Differences in relative antigen (calbindin-D_{28K} or PMCA) expression among chorioallantoic membrane samples from separate embryonic stages were analyzed with a three-factor analysis of variance and Scheffe's multiple comparisons test (SAS 9.2 statistical software). In this analysis, antigen expression was the dependant variable, embryonic stage and blot number were fixed factors, actin immunoreactivity was entered as a covariate, and clutch (female number) used as a random factor.

Table 1. Antibody dilutions and sources.

Primary Antibodies			**Secondary Antibodies**	
Antigen	**Antibody (dilution)**	**Antibody source**	**Antibody (dilution)**	**Antibody source**
Calbindin-D_{28K}	Monoclonal Anti-Calbindin-D_{28K}, Clone CB-955 (1:1000)	Mouse against bovine kidney; Sigma, MO	Biotin-SP-conjugated AffiniPure Goat Anti-Mouse IgG (1:250)	Jackson Laboratories, PA
Calbindin-D_{28K}	Polyclonal Anti-Calbindin-D_{28K} (1:10000)	Rabbit against recombinant corn snake calbindin-D_{28K}; Ecay and Stewart, unpublished	Horseradish-Peroxidase-conjugated Donkey Anti-Rabbit IgG (1:200000)	GE Healthcare, UK
Plasma membrane calcium ATPase (PMCA)	Monoclonal Anti-PMCA, Clone 5F10 (1:2000)	Mouse against human erythrocyte PMCA; Sigma, MO	Horseradish-Peroxidase Sheep Anti-Mouse IgG (1:20000)	GE Healthcare, UK
Actin	Monoclonal Anti-Actin, Clone C4 (1:50000)	Mouse against chicken gizzard actin; Millipore	Horseradish-Peroxidase Sheep Anti-Mouse IgG (1:2000000)	GE Healthcare, UK

RESULTS

Placental Ontogeny

Embryonic stage 31. The maternal–embryonic interface consists of three morphologically distinct regions denoted by extraembryonic membranes; chorioallantoic placenta, choriovitelline placenta and omphaloplacenta. The embryo, enclosed by the amnion, is surrounded by the allantois. The outer allantoic membrane is fused to the chorion, forming the chorioallantoic membrane, around the circumference of the embryonic region of the egg. The chorioallantoic membrane reaches the lateral margins of the yolk sac, but does not extend into the abembryonic hemisphere. The chorioallantoic placenta, defined by apposition of the chorioallantoic membrane and the uterus, is regionally differentiated. The placentome is a specialized region along the mesometrial axis of the egg. This region comprises large, cuboidal chorionic cells and a richly vascularized allantois (Fig. 1). Uterine epithelium of the placentome contains small cuboidal cells often folded in slight ridges in early stages (Fig. 1). The paraplacentome, which surrounds the placentome, contains thin, squamous chorionic cells (Fig. 2). The density of blood vessels in the outer allantoic membrane appears similar throughout the chorioallantoic placenta. Uterine epithelium of the paraplacentome consists of thin, squamous cells (Fig. 2).

A choriovitelline membrane is present between the chorioallantoic placenta and the omphaloplacenta. The chorionic epithelium of this region is thin and squamous, with a highly vascularized mesodermal layer (Fig. 3). The uterine epithelium of the choriovitelline placenta is consists of cuboidal cells and forms ridges in some areas (Fig. 3).

The omphaloplacenta, which extends across the abembryonic hemisphere of the egg, consists of three tissue layers: yolk sac splanchnopleure, omphalopleure and uterine epithelium. The yolk sac splanchnopleure completely surrounds the yolk and consists of an inner layer of endodermal cells with large nuclei and an outer layer of highly vascularized mesoderm. This mesodermal layer is thin, consisting of small squamous cells and larger blood vessels (Fig. 4). A cavity, the yolk cleft, is present between the vascularized splanchnopleure and the outer omphalopleure. The omphalopleure consists of an outer layer of large cuboidal to columnar cells with large, round nuclei and an inner layer of thin squamous cells. This bilayer is overlain by a layer of squamous cells that lines the yolk cleft (Fig. 4). Uterine epithelial cells of the omphaloplacenta are similar to those of the choriovitelline placenta; cells are cuboidal in shape and form ridges in some areas (Fig. 4). Debris is present in the lumen between the uterine and fetal epithelium.

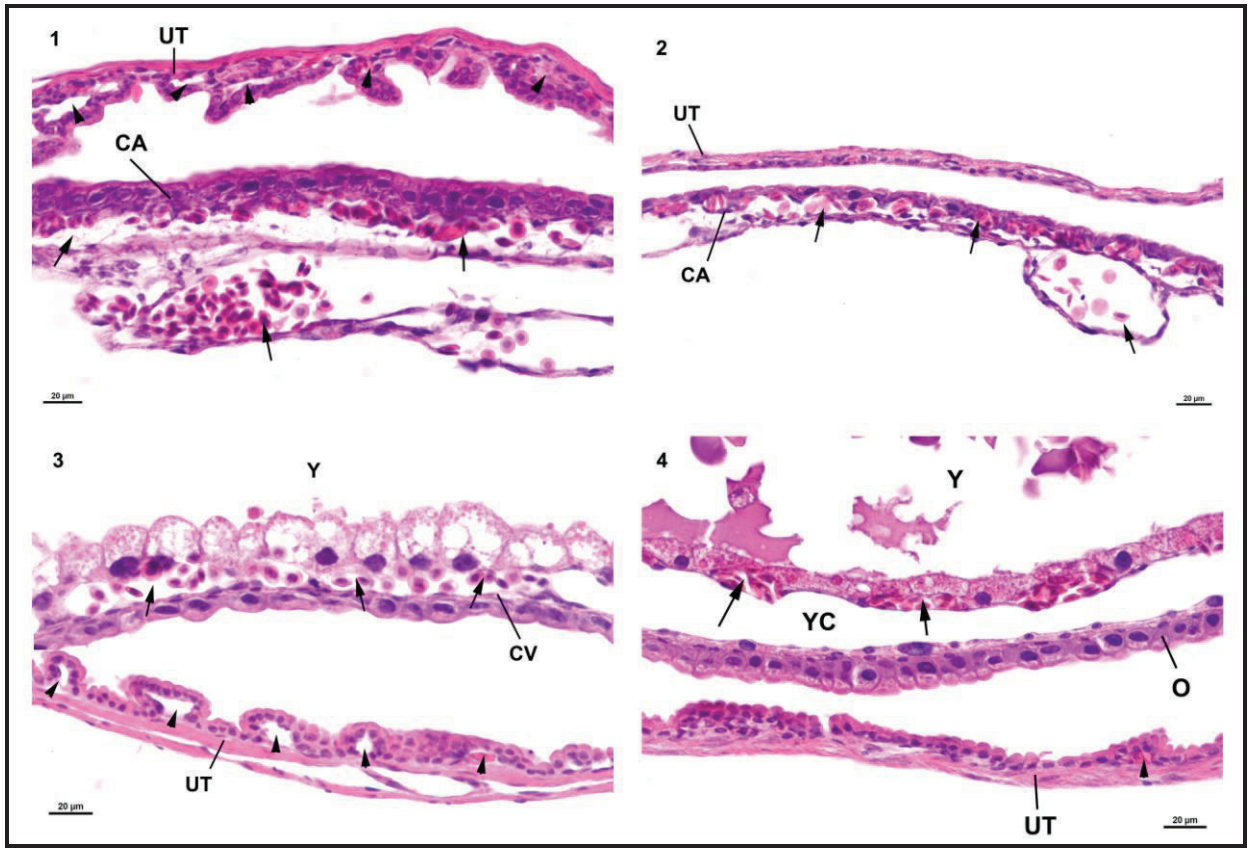

Figure 1. Placentome of the chorioallantoic placenta of a stage 31 embryo. CA, chorioallantoic membrane; UT, uterus; allantoic blood vessels indicated by arrows; uterine blood vessels indicated by arrowheads.
Figure 2. Paraplacentome of the chorioallantoic membrane of a stage 31 embryo. CA, chorioallantoic membrane; UT, uterus; allantoic blood vessels indicated by arrows.
Figure 3. Choriovitelline placenta of a stage 31 embryo. CV, choriovitelline membrane; UT, uterus; Y, yolk vesicle; embryonic blood vessels indicated by arrows; uterine blood vessels indicated by arrowheads.
Figure 4. Omphaloplacenta of a stage 31 embryo. O, omphalopleure; Y, yolk vesicle; YC, yolk cleft; embryonic blood vessels indicated by arrows; uterine blood vessels indicated by arrowheads.

Embryonic stages 33 and 34. The chorioallantoic placenta occupies the embryonic hemisphere of the egg. The placentome is clearly defined and contains large, cuboidal chorionic cells and many blood vessels in the underlying allantois. Uterine epithelium of the placentome consists of folded ridges of small, cuboidal cells. The paraplacentome contains small, squamous

chorionic cells. The allantois is in close proximity to the chorion in both regions and the density of blood vessels is similar throughout the chorioallantoic membrane, as seen in stage 31.
The choriovitelline membrane is visible in stage 33 specimens but is not present in some stage 34 specimens, in which case the upper limit of the omphaloplacenta is delineated by a vascularized array of cells that reaches from the yolk sac splanchnopleure to the chorionic epithelium of the chorioallantoic placenta (Fig. 5). This partition, the interomphalopleuric membrane, blocks the allantois from entering the abembryonic hemisphere.

The morphology of the yolk sac splanchnopleure is similar to stage 31 embryos, but the endodermal cells of the inner layer of the membrane appear larger (Fig. 6). In two stage 33 and one stage 34 specimens, large cells identical to those of the inner layer of yolk sac splanchnopleure are scattered throughout the yolk. The omphalopleure has the same structure as stage 31 embryos (Fig. 7). Uterine epithelium of the omphaloplacenta is cuboidal to columnar in shape and occasionally forms ridges around blood vessels (Fig. 7). Debris is present between the uterine and chorionic epithelium.

Embryonic stages 36 and 37. The relative position of the chorioallantoic placenta in the embryonic hemisphere of the egg is similar to earlier embryonic stages. The embryonic component of the placentome has a similar morphology to stage 34 embryos, but the ridges in the uterine epithelium are more pronounced and appear as highly folded, villus-like projections around a network of blood vessels (Fig. 8). The chorionic cells in the paraplacentome are thin and squamous in shape and are difficult to distinguish overlying the high density of blood vessels in the allantois.

The upper limit of the omphaloplacenta is delineated by the highly vascular interomphalopleuric membrane (Fig. 9). The yolk sac splanchnopleure is similar in structure to

that of stage 34 embryos. The yolk vesicle appears reduced in volume from earlier stages. The fetal epithelium of the omphaloplacenta is similar to previous stages, with an outer layer of large cuboidal to columnar cells of varied heights and two inner cell layers. The apical surface of the outer layer is mostly regular and smooth in stage 36, but some stage 37 specimens exhibit irregularly shaped cells with pointed apical surfaces (Fig. 10). Uterine epithelial cells of the omphaloplacenta are cuboidal in some regions and columnar in others, but all are smaller than apposing fetal epithelial cells. The ridges seen in earlier stages are not as prominent. There is a gradual reduction in height of cells of the uterine epithelium between the abembryonic pole and the lateral margins to the yolk sac, where cells are low cuboidal or squamous. There is much debris in the lumen between the fetal and uterine epithelium.

Embryonic stages 38, 39, and 40. The placentome consists of cuboidal to columnar chorionic cells of varied heights and a highly vascularized allantois. A brush border extends across the apical surface of chorionic epithelial cells of the placentome. As in stage 37 embryos, the uterine epithelium of the placentome is highly folded into villus-like projections around blood vessels. The structure of the paraplacentome is similar to stage 37 embryos.

The yolk vesicle is reduced in volume from earlier stages, pulling away from the outer perimeter of the egg. As a result the interomphalopleuric membrane, which spans this distance, is longer in stage 38 embryos compared to stage 37 and is progressively longer as development advances. The yolk sac splanchnopleure is similar to stage 36 and 37, consisting of large endodermal cells and thin, highly vascularized layer of mesoderm around the entire circumference of the yolk sac. Fetal epithelium of the omphaloplacenta contains three layers and lies exterior to the yolk sac splanchnopleure as seen in stages 36 and 37. The outer epithelial layer consists of large cuboidal cells of varied heights. Some of these cells are irregularly-shaped

and have pointed apical surfaces. The nuclei in such cells are oval-shaped, as opposed to the round shape seen in earlier stages. The morphology of the uterine epithelium is similar to stage 37 embryos. Debris is present between the uterine and fetal epithelium.

Figure 5. Interomphalopleuric membrane of a stage 34 embryo. This partition delineates contact zone between chorioallantoic placenta and omphaloplacenta. The asterisk indicates location of the uterine lumen. AL, allantoic membrane; CA, chorioallantoic membrane; O, omphalopleure; Y, yolk vesicle; arrows indicate embryonic blood vessels.
Figure 6. Yolk sac splanchnopleure and omphalopleure of a stage 33 embryo. Asterisk indicates position of uterine lumen. O, omphalopleure; Y, yolk vesicle; YC, yolk cleft; embryonic blood vessels indicated by arrows.
Figure 7. Omphaloplacenta of a stage 34 embryo. O, omphalopleure; SP, yolk sac splanchnopleure; UT, uterus; Y, yolk vesicle; embryonic blood vessels indicated by arrows; uterine blood vessels indicated by arrowheads.
Figure 8. Uterine epithelium of the placentome of a stage 37 embryo. UT, uterus; arrowheads indicate uterine blood vessels.
Figure 9. Interomphalopleuric membrane of a stage 37 embryo. AL, allantois; CA, chorioallantoic membrane; O, omphalopleure; Y, yolk vesicle; YC, yolk cleft; arrows indicate embryonic blood vessels; asterisk indicates position of uterine lumen.
Figure 10. Irregularly shaped cells in the omphalopleure of a stage 37 embryo. EC, ectoderm; O, omphalopleure; UT, uterus.

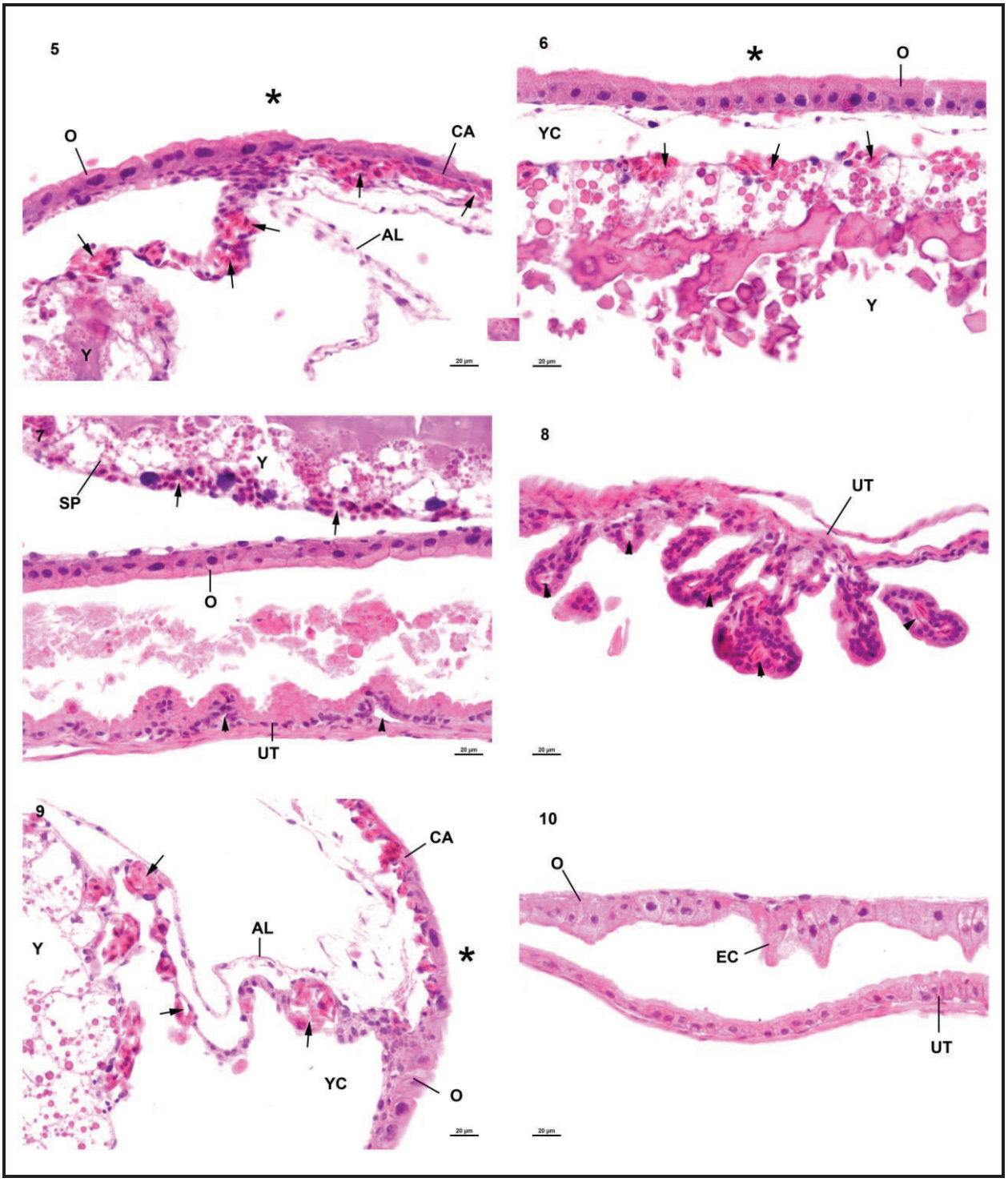
5
*
O
CA
AL
Y
6
*
O
YC
Y
7
SP
Y
O
UT
8
UT
9
CA
AL
Y
*
YC
O
10
O
EC
UT

Calbindin-D_{28K} Immunohistochemistry

Chorioallantoic Placenta: Large cuboidal chorionic cells of the placentome exhibit immune positive staining (brown staining) for calbindin-D_{28K} in all embryonic stages examined (Fig. 12). Staining occurs in patches of adjacent cells in stage 31 specimens (Fig. 11). The staining is most intense in the mid-region of the placentome and lightens in peripheral regions adjacent to the paraplacentome. In later stages (stage 34 onward), the placentome exhibits dark brown staining throughout the outer chorionic cell layer but stops abruptly at the point of contact with the paraplacentome (Fig. 13). The entire cytoplasm of placentome cells stains intensely, but no staining is visible in paraplacentome cells nor in the uterine epithelium in the embryonic hemisphere of the egg (Fig. 12).

Omphaloplacenta: There is scattered immune positive staining in the outer layer of large, cuboidal cells of the fetal epithelium of the omphaloplacenta in early embryonic stages. Staining occurs sporadically, sometimes in small clumps and sometimes in long stretches of adjacent cells (Fig. 14). However, the majority of cells around the perimeter exhibit immune positive staining in stage 38 and older embryos (Fig. 16). Beginning in stage 34, a brush border is evident across the apical surface of the outer layer of fetal epithelium. In cells with reaction product, the brush border stains as intensely as the remainder of the cytoplasm (Fig. 15). After stage 36, the majority of cells in the outer layer of fetal epithelium have a regular, smooth apical surface, but in some specimens there are oddly shaped cells with pointed apical surfaces. There does not seem to be any difference in the pattern of staining in cells with “regular” versus “pointed” apical surfaces.

Embryonic and uterine components of the choriovitelline placenta present in stages 31 and 33 do not exhibit immune positive staining. The interomphalopleuric membrane does not

exhibit brown staining in any stage studied. From stage 33 onward, several specimens from each stage show considerable immune positive staining in the endodermal layer of the yolk sac splanchnopleure around the entire yolk sac (Fig. 16). Uterine epithelium of the omphaloplacenta does not exhibit immune positive staining. Debris in the lumen between the maternal and fetal tissue tends to stain brown.

Figure 11. Placentome of a stage 31 embryo. AL, allantois; CE, chorionic epithelium; UT, uterus; embryonic blood vessels indicated by arrows; uterine blood vessels indicated by arrowheads; DAB staining from calbindin-D_{28K}; hematoxylin counterstain.
Figure 12. Placentome of a stage 34 embryo. AL, allantois; CE, chorionic epithelium; UT, uterus; embryonic blood vessels indicated by arrows; uterine blood vessels indicated by arrowheads.; DAB staining from calbindin-D_{28K}; hematoxylin counterstain.
Figure 13. Junction of paraplacentome and placentome in a stage 40 embryo. AL, allantois; CE, chorionic epithelium; embryonic blood vessels indicated by arrows; asterisk indicates uterine lumen; DAB staining from calbindin-D_{28K}; hematoxylin counterstain.
Figure 14. Omphaloplacenta of a stage 31 embryo. O, omphalopleure; SP, yolk sac splanchnopleure; UT, uterus; Y, yolk vesicle; YC, yolk cleft; embryonic blood vessels indicated by arrows; DAB staining from calbindin-D_{28K}; hematoxylin counterstain.
Figure 15. Omphaloplacenta of a stage 34 embryo. O, omphalopleure; SP, yolk sac splanchnopleure; UT, uterus; Y, yolk vesicle; embryonic blood vessels indicated by arrows. DAB staining from calbindin-D_{28K}; hematoxylin counterstain.
Figure 16. Omphaloplacenta of a stage 40 embryo. O, omphalopleure; UT, uterus; Y, yolk vesicle; YC, yolk cleft; embryonic blood vessels indicated by arrows. DAB staining from calbindin-D_{28K}; hematoxylin counterstain.

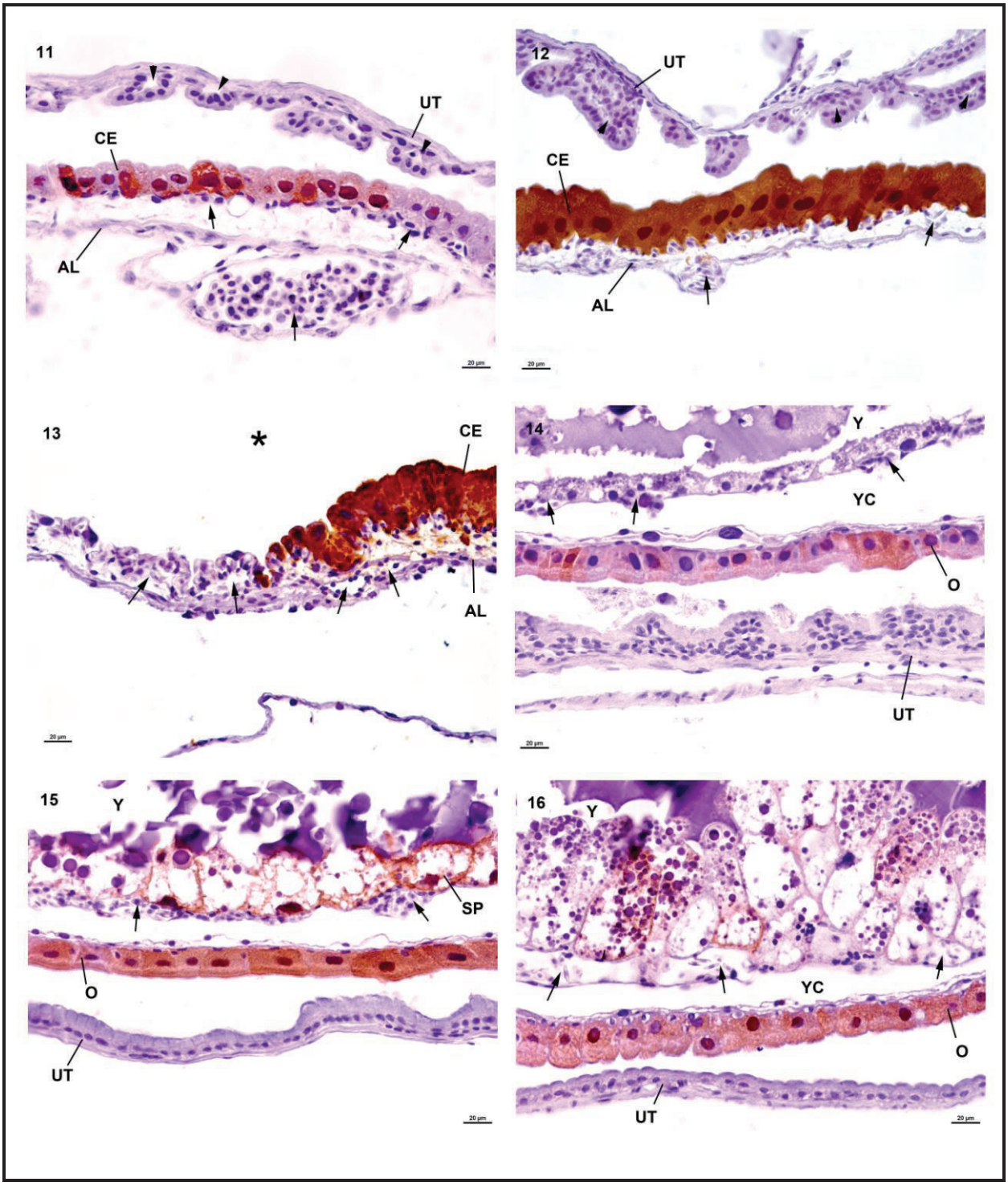
11
UT
CE
AL
12
UT
CE
AL
13
*
CE
AL
14
Y
YC
O
UT
15
Y
SP
O
UT
16
Y
YC
O
UT

Immunoblotting

Actin expression was measured by immunoblotting in the chorioallantoic membrane for all sampled stages of embryonic development. Actin is a component of the cytoskeleton and is consistently expressed in all tissues of all stages of development. Thus, actin serves as a control for protein loading and quantification purposes.

The expression of calbindin-D_{28K} and plasma membrane calcium ATPase (PMCA) were analyzed using immunoblotting methods. Immunoblots (n=10), each with samples from embryonic stages (31-40) reflecting the range of development, were prepared and probed for antigen expression. Stages 31, 34, 36, 37, and 40 were selected for densitometry study, as these stages offered the largest sample sizes and reflect critical stages in the mobilization of calcium. Differences in relative antigen expression were analyzed with a three-factor analysis of variance and Scheffe's multiple comparisons test (Table 2).

Calbindin-D_{28K} expression was low to undetectable in the earliest samples (stage 31) and increased steadily to a peak expression level in stage 40 (Fig. 17). Stage 31 calbindin-D_{28K} expression was significantly different from all other stages analyzed. Stage 34 specimens show strong levels of calbindin-D_{28K} expression, which differed significantly from stage 31 and stage 40 specimens (Fig. 18). Expression during stages 36-40, the peak embryonic growth period, was significantly higher than stage 31. Expression was highest in the final stage before parturition (stage 40). PMCA expression reflected a similar trend (Fig. 19). Expression was low in early stages studied and increased steadily until stage 40 (Fig. 19). A significant difference was observed between stages 31 and 40. Actin expression was consistent for all embryonic stages analyzed.

Table 2. Three-way analysis of variance for the comparison of expression of calbindin-D_{28K} and PMCA between embryonic stages of *Pseudemoia pagenstecheri*.

	Calbindin-D_{28K}		PMCA	
Effect	F Value	*P*	F Value	*P*
Stage	$F_{4,13.9} = 25$	<0.0001	$F_{4, 8.65} = 5.7$	0.015
Blot	$F_{9,39.6} = 7.5$	<0.0001	$F_{9, 35} = 6.9$	<0.0001
Actin	$F_{1, 46.9} = 10.6$	0.002	$F_{1, 47} = 3.98$	0.052

Figure 17. Representative immunoblot for PMCA, calbindin-D_{28K}, and actin during embryonic development in the chorioallantoic membrane of *Pseudemoia pagenstecheri*.

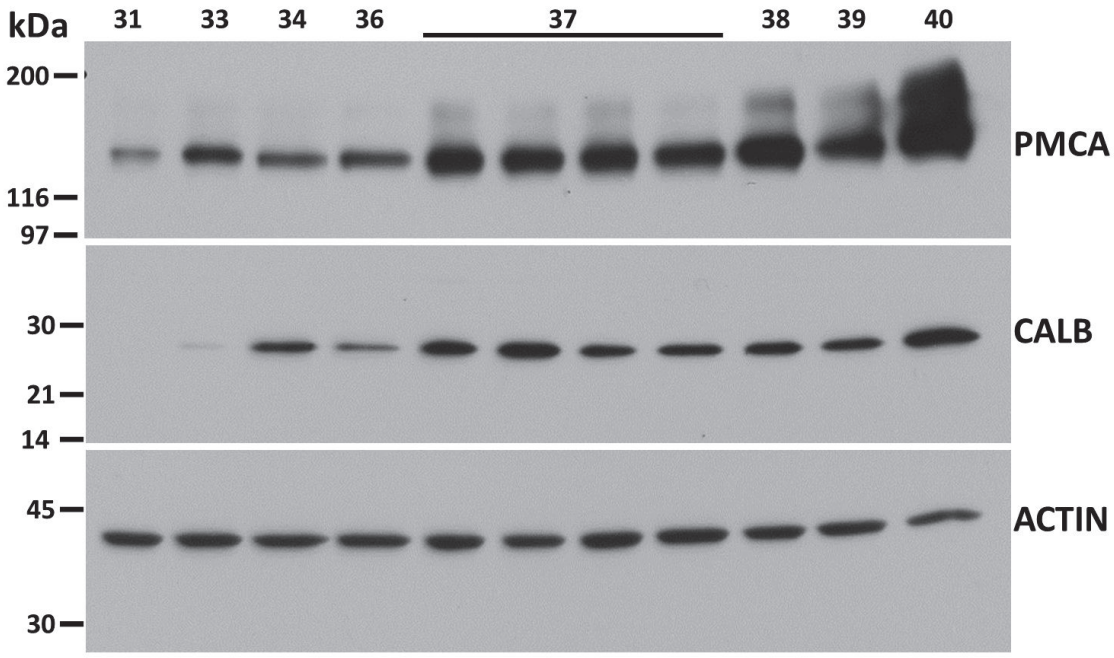

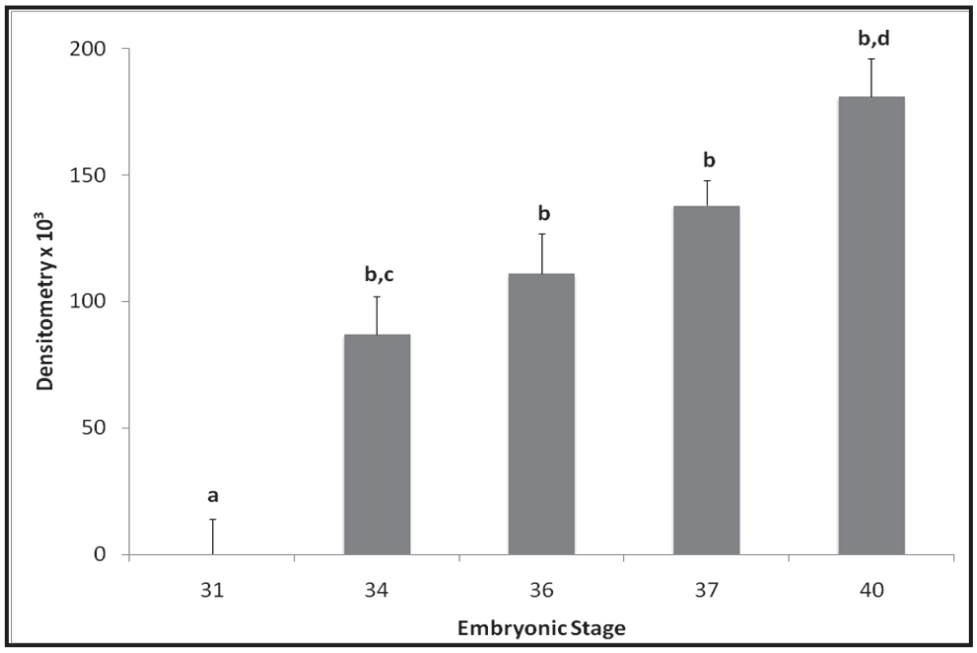

Figure 18. Least squares means of densitometry readings of calbindin-D_{28K} expression during development of *P. pagenstecheri* (differences among means tested with Scheffe's multiple comparison test). Three-way analysis of variance showed significant differences among stages ($F(4,14) = 25$, $P < 0.0001$): a significantly different from b ($P<0.0105$); c significantly different from d ($P\leq0.012$).

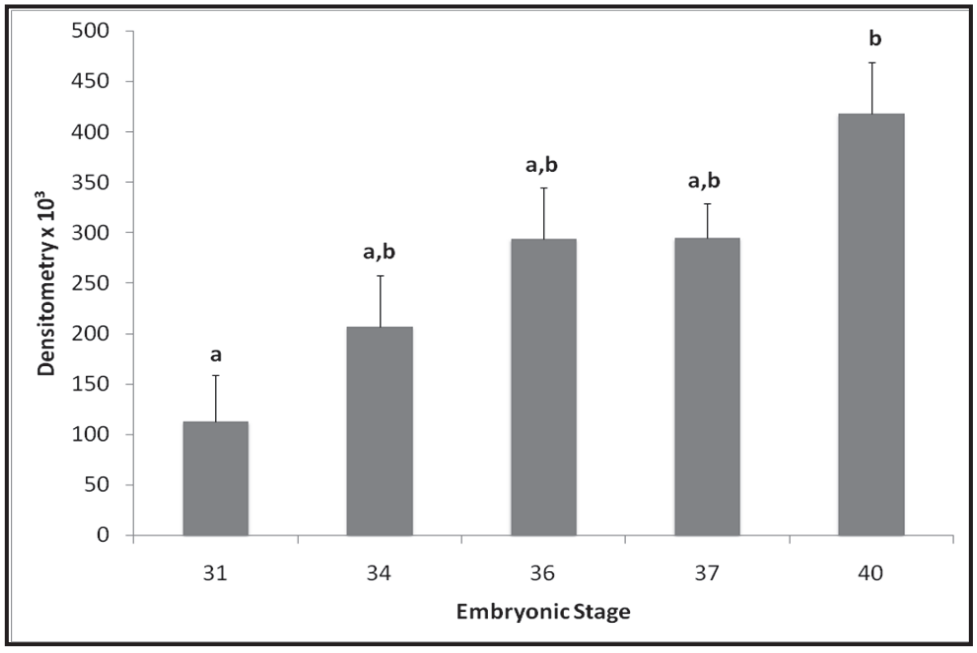

Figure 19. Least squares means of densitometry readings of PMCA expression during development of *P. pagenstecheri* (differences among means tested with Scheffe's multiple comparison test). Three-way analysis of variance showed significant differences among stages ($F(4,8.6) = 5.7$, $P = 0.016$). Stage with the same letter do not differ significantly ($P> 0.05$).

DISCUSSION

Viviparity and Placentation

Complexity of placentation and high levels of placentotrophy, as exhibited by the skinks of the genus *Pseudemoia,* is relatively rare in squamates (Blackburn and Flemming, 2009). Oviparity, or egg-laying, is the ancestral condition for Reptilia, and is characterized by the oviposition of an egg with a calcareous eggshell that develops outside the body. The transition from oviparity to viviparity necessitates a reduction in eggshell thickness (Packard et al., 1977). The loss of a calcified eggshell allows for the intimate apposition of maternal and fetal tissue that facilitates gas and nutrient exchange in the uterus. Within viviparous squamates there is considerable variation in the amount of nutrients supplied to the embryo via placental transfer (Harrison and Weekes, 1925; Weekes, 1935; Blackburn and Flemming, 2009). Placentotrophic species receive the majority of nutrients needed for development via maternal provision across a placenta. In a fully placentotrophic species, the placenta would fulfill all the nutritive, respiratory and excretory needs of the developing embryo (Stewart and Thompson, 2009).

Highly placentotrophic reptile species are rare. Within the order Squamata (lizards and snakes) viviparity has arisen in more than 100 lineages, but placentotrophy has only been documented in four or five lineages of scincid lizards (Blackburn and Flemming, 2009). These species ovulate eggs with small yolks and transfer via placental membranes supplies the majority of nutrients for development (Blackburn and Flemming, 2009). Placentotrophic species of these lineages exhibit elaboration of fetal and maternal tissues (Blackburn and Flemming, 2009). However, the role of these membranes in the transfer of nutrients, that is, the functional mechanisms for transport in these tissues, is not well understood.

Placental ontogeny in the genus *Pseudemoia*

All reptiles have homologous fetal membranes: an amnion, chorioallantois, and yolk sac (Blackburn and Flemming, 2009). Placentas form in viviparous squamates as the extraembryonic membranes of the chorioallantois and yolk sac come in direct contact with maternal tissue of the uterus (Blackburn and Flemming, 2009). Apposition of the uterus to extraembryonic membranes of the yolk sac constitutes the yolk sac placenta (Blackburn, 1993). Apposition of the uterus to the choriovitelline membrane, bilaminar omphalopleure or omphallallantoic membrane constitutes the three classes of yolk sac placentae: choriovitelline placenta, omphaloplacenta, and omphallantoic placenta, respectively (Stewart and Blackburn, 1988). All viviparous squamates have chorioallantoic placentae (Stewart et al., 2009[b]). The chorioallantoic placenta results from simple apposition of the chorioallantois (and in some cases, including overlying shell membrane) to the inner lining of the uterus (Blackburn, 1993). Viviparous squamates exhibit a range of diversity in the complexity of fetal and maternal tissue.

In her classic work on reptilian allantoplacentation, Weekes (1935) described three placental morphotypes based on the structure of uterine and chorionic tissues at the maternal-embryonic interface. The simplest and most common type of placenta was deemed Type I (Weekes, 1935). A Type I placenta is characterized by close apposition of maternal and embryonic epithelial tissue (chorioallantois) (Weekes, 1935). The most complex placenta under Weekes' (1935) classification was Type III, which is characterized by a highly specialized area of apposed, folded maternal and fetal tissues, that is, the placentome. The three species of *Pseudemoia* studied to date are all classified as Type III. Weekes based this placental morphotype on work done on "*Lygosoma (Liolepisma) entrecasteauxii*" (Harrison and Weekes, 1925; Weekes, 1930) and "*Lygosoma (Liolepisma) weekesae*" (Weekes, 1929). The taxonomy of

"*Liolepisma entrecasteauxii*" was later revised by recognition of three species (*P. entrecasteauxii*, *P. pagenstecheri*, and *P. cryodroma*), which were placed in the genus *Pseudemoia* (Hutchinson and Donnellan, 1992). *Pseudemoia entrecasteauxii* and *P. pagenstecheri* are both included in the original descriptions of Type III placentation (Thompson and Stewart, 1998). The identity of *L. weekesae* is uncertain, but is now thought to be *P. spenceri* based on collection location and placental ontogeny, which is consistent with Weeke's (1935) Type III placenta (Stewart and Thompson, 1998).

These three *Pseudemoia* species (*P. entrecasteauxii, P. pagenstecheri,* and *P. spenceri*) are also characterized by the compartmentalization of embryonic and abembryonic hemispheres of the egg. The allantois is blocked from entering the abembryonic portion of the egg by a vascularized membrane that stretches from the bilaminar omphalopleure to the yolk sac splanchnopleure called the interomphalopleuric membrane (Stewart and Thompson, 1998, 2003). Similar partitions have been described in *Niveoscincus metallicus* (Stewart and Thompson, 1994) and *Chalcides chalcides* (Blackburn, 1993), but this pattern of modification of the egg is uncommon among squamates (Stewart, 1993).

In early development, two placental structures are present in the embryonic hemisphere of *Pseudemoia* eggs: the chorioallantoic placenta, which will be the terminal placental structure in the embryonic hemisphere, and the temporary choriovitelline placenta, which regresses as development proceeds. The chorioallantoic placenta covers most of the embryonic hemisphere of the egg by stage 31 (Stewart and Thompson, 1996, 2003). The choriovitelline membrane is confined to the lateral margins of the yolk sac. Timing of replacement of the choriovitelline membrane of *P. spenceri* occurs by stage 34 or 35, but is accelerated in *P. entrecasteauxii* and occurs prior to embryonic stage 32 (Stewart and Thompson, 1996, 2003).). In *P. pagenstecheri*

replacement of the choriovitelline membrane occurs by stage 34 or 35. The uterine epithelium in all three species consists of low, cuboidal cells, but the epithelium is highly folded in *P. spenceri* (Stewart and Thompson, 1998, 2003). Uterine epithelium in *P. pagenstecheri* is also folded into ridges in some areas. This similarity is interesting as it is not observed in *P. entrecasteauxii* or other squamates.

The chorioallantoic membrane is confined to the embryonic hemisphere of the egg in all three species of *Pseudemoia*. Differentiation of the chorioallantoic membrane into placentomal and paraplacentomal regions is evident in all three species in embryonic stages 30-31 (Stewart and Thompson 1996, 2003). The basic morphology of the chorioallantois is similar in all three species. Dorsal to the embryo, a well-defined region called the placentome consists of hypertrophied chorionic and uterine epithelium supported by rich vascularization. Chorionic epithelium consists of large, cuboidal cells supported by a densely vascularized allantois (Fig.1). Uterine epithelium is comprised of cudoidal cells folded into prominent ridges. In all three species, this morphology persists throughout gestation, but chorionic cells increase in size as development proceeds. The ridges in apposing uterine tissue also become more pronounced in later stages of development.

The remainder of the chorioallantoic membrane, the paraplacentome (Fig. 2), stretches from the placentome to the omphaloplacenta. In all three species this structure is defined by thin, squamous chorionic and uterine epithelium comprised of much smaller cells than those of the placentome. This region is highly vascularized. Expansion of the allantois into the abembryonic hemisphere of the egg is blocked by the development of the interomphalopleuric membrane, a structure derived from intravitelline cells (Stewart and Thompson, 2003). This membrane initially manifests as a small, vascularized mass of cells and expands into a sheet of tissue

connecting the bilaminar omphalopleure to the yolk sac splanchnopleure. The structure persists throughout gestation, blocking the allantois from invading the abembryonic hemisphere of the egg.

In all three species the omphaloplacenta occupies the abembryonic hemisphere of the egg. In stage 30-31 *P. spenceri* embryos, a thin, but intact, isolated yolk mass is present (Stewart and Thompson, 1998, 2003), whereas the isolated yolk mass in stage 30 *P. entrecasteauxii* embryos is present only as scattered remnants of small yolk platelets (Stewart and Thompson, 1996). Remnants of an isolated yolk mass were not visible in any stage 31 *P. pagenstecheri* specimens observed. Morphology of the mature omphaloplacenta is similar in the three species. Embryonic epithelium is comprised of three layers. The outermost layer is cuboidal to columnar across the entire surface of the omphaloplacenta in *P. pagenstecheri* and *P. entrecasteauxii*, and most of the surface in *P. spenceri* (Stewart and Thompson, 2003). The inner layer is thin and squamous. A third layer of cells is sparsely distributed across the surface of the inner squamous layer of the epithelium in all three species (Stewart and Thompson, 1996, 1998, 2003). The yolk sac splanchnopleure is highly vascularized across the entire surface of the yolk sac in *P. entrecasteauxii* and *P. pagenstecheri*, but blood vessels are not present near the abembryonic pole in *P. spenceri* (Stewart and Thompson, 1998). The uterine epithelium of the omphaloplacenta is cuboidal to columnar and folded into ridges in some places around blood vessels.

The development and structure of placental membranes in the three species of *Pseudemoia* described above are similar. The three species share the same set of morphologically elaborated tissues, albeit some minor differences in timing of development relative to embryonic

stage and in structure. As the placental structure is similar, we should expect to observe similar functional specializations in the three species.

Functional attributes in *Pseudemoia*

The three species of *Pseudemoia* studied to date exhibit similarity in placental structure and all demonstrate high levels of placentotrophy (Stewart and Thompson, 1993; Thompson and Stewart, 1994; Thompson et al., 1999). We know placentotrophic species depend on maternal provision of nutrients because neonatal dry mass exceeds that of recently ovulated eggs. The egg to neonate dry mass ratio is 1.23 in *P. spenceri* (Thompson et al., 1999), 1.7 in *P. entrecasteauxii* (Stewart and Thompson, 1993) and 2.4 in *P. pagenstecheri* (Thompson et al., 1999[b]). Furthermore, neonates of all three species contain significantly more calcium, sodium and potassium than recently ovulated eggs, indicating substantial transfer of ions (Stewart and Thompson, 1993; Thompson and Stewart, 1994; Thompson et al., 1999[b]). Differences exist in the ion content of neonates of each species, indicating some variation in the placental transfer of ions (Thompson et al., 1999[b]). Extensive transfer of nutrients occurs in all three species but the mechanism of transfer from mother to embryo is not well understood.

Structural studies in *P. entrecasteauxii* indicate the uterus plays a role in nutrient transfer in the omphaloplacenta (Adams et al., 2005). Cytological features of the uterine portion of the omphaloplacenta indicate that the region is a site of histotrophic nutrient transfer (Adams et al., 2005). The presence of hypertrophied, active secretory cells in association with electron-dense granules and abundant vesicles pinching off from the uterine epithelium cells implicate the omphaloplacenta as a site of active histotrophic secretion in *P. entrecasteauxii* (Adams et al., 2005). Study of a membrane-bound enzyme, alkaline phosphatase, correlated with transcellular

transfer of nutrients in the uterus of *P. entrecasteauxii* and *P. spenceri* found expression of the protein on the apical plasma membrane of uterine epithelial cells in the omphaloplacenta (Biazek et al., 2010). There is a strong correlation between alkaline phosphatase activity and sites of secretion, including active transport of lipids across plasma membranes (DeSchryver-Kecskemeti et al., 1991). Biazek et al. (2010) suggests that active transport processes may be at work in the transfer of lipids and glucose across the plasma membrane in viviparous skinks. It appears there are several mechanisms of transfer in place in the uterine omphaloplacental tissue of skinks and further work will clarify such processes.

Further, morphological comparisons indicate different roles for the uterine epithelium of the paraplacentome versus that of the placentome (Adams et al., 2005). Cytological modifications required for gas exchange and histotrophy are incompatible. Maximum gas exchange requires thin uterine epithelium whereas histotrophic transfer is facilitated by secretion by enlarged epithelial cells (Blackburn, 1993). Cytological features of the uterine epithelium of the paraplacentome indicate that this site is associated with gaseous exchange (Adams et al., 2005). The maternal portion of the placentome has different cytological properties from the paraplacentome. Cytology of the uterine epithelium is similar to that of the omphaloplacenta, but lacks electron-dense granules and apocrine secretions pinching off the maternal tissue (Adams et al., 2005). While the secretory mechanism of the placentome is uncertain, it is still implicated in histotrophic transport, possibly via mechanisms other than apocrine secretion (Adams et al., 2005).

Work on the functional capability of embryonic epithelial cells in the placentome and the omphaloplacenta of *P. entrecasteauxii* indicates that these cells are capable of non-specific endocytosis (Stewart et al., 2006). These cells can take up moderately-sized molecules (Stewart

et al., 2006), an observation consistent with the suggestion that these two placental regions transport secretions from the uterine epithelium (Stewart and Thompson, 1996; Adams et al., 2005). *Pseudemoia pagenstecheri* exhibits similar structural differentiation to *P. entrecasteauxii* and the functional capabilities of uterine and fetal tissue are expected to be similar as well.

The mechanism for calcium transfer across the placenta in squamates is yet unknown and either maternal or embryonic tissues may regulate calcium delivery (Thompson et al., 1999[a]). The pattern of calcium provision to embryos of the three species of *Pseudemoia* suggests that both maternal and embryonic systems may be involved in the placental provision of calcium (Thompson et al., 1999[a]). All three species are placentotrophic for calcium transport. Neonate to egg calcium content ratios in the three species are as follows: 2.4 in *P. spenceri* (Thompson et al.,1999[a]), 3.6 in *P. entrecasteauxii* (Stewart and Thompson, 1993), and 10.4 in *P. pagenstecheri* (Thompson et al., 1999[b]). *Pseudemoia pagenstecheri* exhibits the highest level of calcium placentotrophy of the three species, with 90% of neonate calcium supplied by maternal transfer (Thompson et al., 1999[b]).

Calcium Acquisition Patterns

The pattern of calcium mobilization of viviparous squamate embryos is similar to oviparous species as the embryonic uptake of calcium is correlated with embryonic growth (Stewart and Ecay, 2010). The extraction of calcium from the eggshell and placental transfer of calcium both occur late in development, during the peak embryonic growth period (Stewart and Ecay, 2010). The review of patterns of maternal provision and embryonic mobilization of calcium in squamates by Stewart and Ecay (2010) supplied an ontogenetic pattern of calcium mobilization by oviparous embryos based on six oviparous lizards and three oviparous snakes

(Packard et al., 1984, 1985, 1992; Packard and Packard 1988; Shadrix et al., 1994; Stewart et al., 2004, 2009[a,b]; Linville et al., 2010). Little change in dry mass or calcium distribution in yolk, embryo or shell occurs during early embryonic stages (Stewart and Ecay, 2010). Following embryonic differentiation, a dramatic increase in embryonic dry mass is observed, in concert with a decrease in yolk dry mass (Stewart and Ecay, 2010). Calcium content in the embryo increases as dry mass increases. Embryonic calcium gains during the first phase of growth result from exploitation of yolk calcium, as the total calcium content of the embryo and yolk remains constant (Stewart and Ecay, 2010). In later development, prior to hatching, calcium is extracted from the eggshell, a trend that accounts for a total calcium content in the egg that exceeds the quantity in oviposited eggs (Stewart and Ecay, 2010). In oviparous lizards of the family Scincidae, for instance, 39-57% of hatchling calcium content is extracted from the eggshell (Thompson et al., 2000). The amount of calcium in the yolk continues to drop throughout the embryonic growth phase, indicating that eggshell calcium is taken up directly by the embryo and not stored in the yolk (Stewart and Ecay, 2010).

Comparison of the pattern of calcium mobilization in *P. pagenstecheri* with an oviparous skink, *Saproscincus mustelinus,* reveals a departure from the pattern of calcium mobilization evident in most oviparous squamates (Stewart et al., 2009[a]). Calcium concentration in the yolk of stage 31 embryos is similar to *S. mustelinus*, but calcium mobilization from the yolk is initiated earlier in *P. pagenstecheri* (Stewart et al., 2009[a]). The pattern of embryonic calcium mobilization during the peak embryonic growth phase (stages 36-40) follows a similar pattern as *S. mustelinus*, but placental transfer of calcium to *P. pagenstecheri* greatly exceeds calcium recovery from the eggshell in *S. mustelinus* (Stewart et al, 2009[a]; Stewart and Ecay, 2010). As a result, neonatal *P. pagenstecheri* embryos have a higher calcium concentration than hatchling *S.*

mustelinus (Stewart et al., 2009[a]). The greater neonate calcium concentration indicates specialized placental structures in *P. pagenstecheri* have a functional significance in calcium transport (Stewart et al., 2009[a]).

Mechanisms of Calcium Transport

So how is calcium transported to the developing embryo in viviparous species? Few studies have investigated the mechanisms of calcium transport across maternal and embryonic tissues of squamates, oviparous or viviparous. Our current understanding of calcium transfer is largely based on studies of the calcium-transporting properties of homologous reproductive and embryonic tissue in chickens and other avian species, which were often modeled on other avian and vertebrate tissues and organs involved in calcium homeostasis (Stewart and Ecay, 2010).

Calbindin-D_{28K} is a cytosolic calcium-binding protein that aids in transcellular transport (Bindels, 1993). Calbindin-D_{28K} has been correlated with calcium transport activity in a variety of tissues (Feher et al., 1992; Bindels, 1993), including the chorioallantoic membrane and yolk sac of an oviparous snake (Ecay et al., 2004). Released from calbindin, calcium crosses the basolateral plasma membrane facilitated by Ca^{2+} ATPase (Wasserman et al., 1992; Bronner and Pansu, 1999). Plasma membrane Ca^{2+} ATPase (PMCA) expression has been studied in the uterine tissue of lizard species, both oviparous and viviparous, with varying levels of placentation, including two other species of the genus *Pseudemoia* (Herbert et al., 2006, Herbert et al., 2010). PMCA has an integral role in providing calcium ions for egg-shelling, and shell glands were found to developmentally regulate expression of PMCA to coincide with calcification of the eggshell in an oviparous lizard species, in early stages of development (Herbert et al., 2006). Viviparous species with simple placental structures also show expression

of PMCA during early stages of development (Herbert et al., 2006). However, in species with complex placentae, *Pseudemoia spenceri* and *P. entrecasteauxii*, Ca^{2+} ATPase pumps were expressed through pregnancy (Herbert et al., 2010). This prolonged expression of Ca^{2+} ATPase pumps provides a direct means to provide calcium to the embryo throughout development, but particularly when demand is greatest during late embryonic stages (Herbert et al., 2010).

Calbindin-D_{28K} was expressed in the embryonic epithelium of the omphaloplacenta and in the chorionic epithelium of the placentome, but not in the remainder of the chorioallantoic placenta in *Pseudemoia pagenstecheri*. Expression of calbindin-D_{28K} was observed in these membranes throughout development, as indicated by both immunohistochemical and western blot data. Western blot data also indicates PMCA is expressed in the chorioallantoic membrane throughout development. Thus, calcium transport is occurring over an extended interval of gestation. Furthermore, calbindin-D_{28K} and PMCA expression levels are highest during stages 36-40, when *P. pagenstecheri* embryos mobilize a substantial mass of calcium, mostly from placental transfer (Stewart et al., 2009). Expression of calbindin-D_{28K} in specialized regions of the extraembryonic membranes during the developmental interval of peak embryonic uptake of calcium implicates these regions as sites of calcium transport. This indicates that these structures are playing some role in calcium transport; the structural elaboration has a functional component. Calcium transport is at least one functional attribute of these structurally elaborate regions in the chorioallantoic placenta and omphaloplacenta.

Implications for Placental Evolution

The transition from oviparity to viviparity must be accompanied by a reduction in eggshell thickness to facilitate gas exchange. Packard et al. (1977) suggested that if an embryo

relies on the calciferous layer of the eggshell as a source of calcium during development, the requisite loss of the eggshell in the transition to viviparity would leave the embryo nutritionally deficient. This hypothesis is premised on the observation that exclusively oviparous amniote lineages such as crocodiles, birds and turtles are highly dependent on eggshell calcium whereas in the lizards and snakes, a clade in which viviparity has evolved multiple times, embryos depend primarily on yolk calcium content (Packard et al., 1977). This model suggests that viviparity will evolve in lineages that have calcium-rich yolk and embryos who do not depend on eggshell calcium (Stewart and Ecay, 2010). This suggestion has been proven false, as several lineages of oviparous squamates extract calcium from the eggshell during development, including those with viviparous species or populations (Stewart and Thompson, 1993; Shadrix et al., 1994; Thompson et al., 2001; Stewart et al., 2009[a,b]; Linville et al., 2010). However, comparisons of oviparous and viviparous populations of the reproductively bimodal lizards *Saiphos equalis* and *Zootoca vivipara* indicate viviparous populations may in fact have a nutritional deficiency compared to oviparous populations when it comes to calcium (Stewart et al, 2009[b]; Linville et al., 2010). The viviparous populations of both species exhibit substantial levels of placental calcium transfer, some 76% of neonatal calcium in *Z. vivipara* and 28% in *S. equalis* (Stewart et al, 2009[b]; Linville et al., 2010). In both species, viviparous neonates have lower calcium densities than oviparous hatchlings (Stewart et al, 2009[b]; Linville et al., 2010). No differences in ontogeny or structure of extraembryonic membranes are evident between oviparous and viviparous populations of *Z. vivipara* (Stewart et al., 2009[b]). The relative contribution of placental calcium to neonates (76%) is comparable to species that have structurally specialized placentae, such as *Pseudemoia pagenstecheri* (Stewart et al., 2009[b]). Morphological specializations are not required for substantial amounts of placental calcium

transfer. However, in the absence of such elaboration placental calcium transfer is less effective than embryonic extraction from an eggshell (Stewart and Ecay, 2010). Thus, the evolution of placental specializations for calcium transfer may function to overcome calcium deficits and allow placental transfer of calcium to be as effective as calcium extraction from the eggshell.

Structural specialization of the chorioallantoic placenta, similar to the placentome of *P. pagenstecheri*, has evolved independently in another genus of scincid lizards, the genus *Mabuya* (Blackburn et al., 1984). In viviparous species of *Mabuya* a placentome forms dorsal to the embryo, consisting of hypertrophied uterine and embryonic tissue (Blackburn and Vitt, 1992). Recent study shows the expression of calbindin-D_{28K} in the chorionic epithelium of the placentome of *Mabuya sp.* (Wooding et al., 2010) indicating independently derived similarity (homoplasy) in both structural and functional placental specialization. The placentome is a calcium-transporting region in two viviparous skink species and further work in squamates with similar complexity of placental structure will provide valuable information about the relationship between structure and function in squamate placentas.

WORKS CITED

Adams SM, Biazik JM, Thompson MB, Murphy CR. 2005. *Cyto*-epitheliochorial placenta of the viviparous lizard *Pseudemoia entrecasteauxii*: a new placental morphotyope. J Morphol 264:264-276.

Biazik JM, Thompson MB, Murphy CR. 2010. Paracellular and transcellular transport across the squamate uterine epithelium. Herpetol Conserv Biol 5:257-262

Bindels RJM. 1993. Calcium handling by the mammalian kidney. J Exp Biol 184:89-104.

Blackburn DG. 1982. Evolutionary origins of viviparity in the Reptilia. I. Sauria. Amphibia-Reptilia 3:259-291.

Blackburn DG. 1985. Evolutionary origins of viviparity in the Reptilia. II. Serpentes, Amphisbaenia, and Ichthyosauria. Amphibia-Reptilia 5:529-291.

Blackburn DG. 1992. Convergent evolution of viviparity, matrotrophy, and specializations for fetal nutrition in reptiles and other vertebrates. Am Zool 32:313-321.

Blackburn DG. 1993. Chorioallantoic placentation in squamate reptiles: structure, function, development, and evolution. J Exp Zool 266:414-430.

Blackburn DG. 2006. Squamate reptiles as model organisms for the evolution of viviparity. Herpetol Monographs 20:131-146.

Blackburn DG, Flemming AF. 2009. Morphology, development, and evolution of fetal membranes and placentation in squamate reptiles. J Exp Zool (Mol Dev Evol) 312B:579-589.

Blackburn DG, Vitt LJ. 1992. Reproduction in South American lizards of the genus *Mabuya*. In. Hamlett W, editor. Reproductive biology of South American vertebrates: aquatic and terrestrial. New York: Springer-Verlag; p. 150-164.

Blackburn DG, Vitt LJ , Beuchat CA. 1984. Eutherian-like reproductive specializations in a viviparous reptile. Proc Natl Acad Sci USA 81:4860–4863.

Bronner, F., Pansu, D. 1999. Nutritional aspects of calcium absorption. J. Nutr. 129: 9-12.

Dufaure JP, Hubert J. 1961. Table de developpement du lizard vivipara: Lacerta (Zootoca) vivpara Jacquin. Arch Anat Micros Morphol Exp 50:309-328.

DeSchryver-Kecskemeti K, Eliakim R, Green K, Alpers DH. 1991. A novel intracellular pathway for rat intestinal digestive enzymes (alkaline phosphatase and sucrose) via a lamellar particle. J Soc Gynecol Invest 4:23-30.

Ecay TW, Stewart JR, Blackburn DG. 2004. Expression of calbindin-D_{28k} by yolk sac and chorioallantoic membranes of the corn snake, *Elaphe guttata.* J Exp Zool (Mol Dev Evol) 302B:517-525.

Feher JJ, Fullmer CS, Wasserman RH. 1992. Role of facilitated diffusion of calcium by calbindin in intestinal calcium absorption. Am J Physiol Cell Physiol 262:C517-C526.

Harrison L, Weekes HC. 1925. On the occurrence of placentation in the scincid lizard, *Lygosoma entrecasteauxii*. Proc Linn Soc NSW 50:470-486.

Herbert JF, Lindsay LA, Murphy CR, Thompson MB. 2006. Calcium transport across the uterine epithelium of pregnant lizards. Herp Monographs 20:205-211.

Herbert JF, Murphy CR, Thompson MB. 2010. Calcium ATPase localization in the uterus of two species of *Pseudemoia* (Lacertilia: Scincidae) with complex placentae. Herpetol Conserv Biol 5(2):290-296.

Hutchinson MN, Donnellan SC. 1992. Taxonomy and genetic variation in the Australian lizards of the genus *Pseudemoia* (Scincidae:Lygosominae). J Nat Hist 26:215-264.

Laemmli UK. 1970. Cleavage of structural proteins during the assembly of the head of bacteriophage T4. Nature 227:680-685.

Linville BJ, Stewart JR, Ecay TW, Herbert JF, Parker SL, Thompson MB. 2010. Placental calcium provision in a lizard with prolonged oviductal egg retention. J Comp Physiol B 180:221-227.

Packard GC, Tracy CR, Roth JJ. 1977. The physiological ecology of reptilian eggs and embryos, and the evolution of viviparity within the Class Reptilia. Biol Rev 52:71-105.

Packard MJ, Packard GC. 1988. Sources of calcium and phosphorus during embryogenesis in Bullsnakes (*Pituophis melanoleucus*). J Exp Zool 246:132-138.

Packard MJ, Packard GC, Gutzke WHN. 1984. Calcium metabolism in embryos of the oviparous snake *Coluber constrictor.* J Exp Biol 110:99-112.

Packard MJ, Packard GC, Miller JD, Jones ME, Gutzke WHN. 1985. Calcium mobilization, water balance, and growth in embryos of the agamid lizard *Amphibolurus barbatus*. J Exp Zool 235:349-357.

Packard MJ, Phillips JA, Packard GC. 1992. Sources of mineral for Green Iguanas (*Iguana iguana*) developing in eggs exposed to different hydric environments. Copeia 1992:851-858.

Shine, R. 1985.The evolution of viviparity in reptiles: an ecological analysis. In *Biology of the Reptilia,* vol. 15 (eds. C. Gans and F. Billett), pp. 605-694. New York: John Wiley and Sons.

Shadrix CA, Crotzer DR, McKinney SL, Stewart JR. 1994. Embryonic growth and calcium mobilization in oviposited eggs of the scincid lizard, *Eumeces fasciatus*. Copeia 1994:493-498.

Smith SA. 2001. A molecular phylogenetic study of the Eugongylus group of skinks. Ph.D. dissertation, University of Adelaide, Adelaide, Australia.

Stewart JR. 1993. Yolk sac placentation in reptiles: structural innovation in a fundamental vertebrate fetal nutritional system. J Exp Zool 266:431- 449.

Stewart JR, Blackburn DG. 1988. Reptilian placentation: structural diversity and terminology. Copeia 1988:839-852.

Stewart JR, Ecay TW. 2010. Patterns of maternal provision and embryonic mobilization of calcium in oviparous and viviparous squamate reptiles. Herpetol Conserv Biol 5(2):341-359.

Stewart JR, Thompson MB. 1993. A novel pattern of embryonic nutrition in a viviparous reptile. J Exp Biol 174:97-108.

Stewart JR, Thompson MB. 1996. Evolution of reptilian placentation: development of extraembryonic membranes of the Australian scincid lizards, *Bassiana duperreyi* (oviparous) and *Pseudemoia entrecasteauxii* (viviparous). J Morphol 227:349-370.

Stewart JR, Thompson MB. 1998. Placental ontogeny of the Australian scincid lizards *Niveoscincus coventryi* and *Pseudemoia spenceri*. J Exp Zool 282:535-559.

Stewart JR, Thompson MB. 2000. Evolution of placentation among squamate reptiles: recent research and future directions. Comp Biochem Physiol A 127:411-431.

Sewart JR, Thompson MB. 2003. Evolutionary transformations of the fetal membranes of viviparous reptiles: a case study of two lineages. J Exp Biol 299A:13-32.

Stewart JR, Thompson MB. 2009. Parallel evolution of placentation in Australian scincid lizards. J Exp Biol (Mol Dev Evol) 310B:590-602.

Stewart JR, Thompson MB, Attaway MB, Herbert JF, Murphy CR. 2006. Uptake of dextran-FITC by epithelial cells of the chorioallantoic placentome and the omphalopleure of the placentotrophic lizard, *Pseudemoia entrecasteauxii*. J Exp Biol 305A:883-889.

[a]Stewart JR, Ecay TW, Garland CP, Fregoso SP, Price EK, Herbert JF, Thompson MB. 2009. Maternal provision and embryonic uptake of calcium in an oviparous and a placentotrophic Australian lizard (Lacertilia: Scinidae). Comp Biochem Physiol A 153:202-208.

[b]Stewart JR, Ecay TW, and Heulin B. 2009. Calcium Provision to oviparous and viviparous embryos of the reproductively bimodal lizard *Lacerta (Zootoca) vivipara.* J Exp Biol. 212:2520-2524.

Thompson MB, Stewart JR. 1994. Egg and clutch size of the viviparous Australian skink, *Pseudemoia pagenstecheri* and the identity of species with type III allantoplacentae. J Herpetol 28:519-521.

[a]Thompson MB, Stewart JR, Speake BK, Russell KJ, McCartney RJ. 1999. Placental transfer of nutrients during gestation in the viviparous lizard, *Pseudemoia spenceri.* J Comp Physiol B 169:319-328.

[b]Thompson MB, Stewart JR, Speake BK, Russell KJ, McCartney RJ, Surui PF. 1999. Placental nutrition in a viviparous lizard (*Pseudemoia pagenstecheri*) with a complex placenta. J Zool (Lond) 248:295-305.

Thompson MB, Stewart JR, Speake BK. 2000. Comparison of nutrient transfer across the placenta of lizards differing in placental complexity. Comp Biochem Physiol A 127:469-479.

Thompson MB, Speake BK, Russell KJ, McCartney RJ. 2001. Utilization of lipids, proteins, ions, and energy during embryonic development of Australian oviparous skinks in the genus *Lampropholis*. Comp Biochem and Phys A 129:313-326.

Tuan RS. 1984. Carbonic anhydrase and calcium transport function of the chick embryonic chorioallantoic membrane. Annals of the New York Academy of Sciences 429: 459-472.

Towbin H, Staehelin T, Gordon J. 1979. Electrophoretic transfer of proteins from polyacrylamide gels to nitrocellulose sheets: procedure and some applications. Proc Natl Acad Sci USA 76:4350-4354.

Wasserman RH, Chandler JS, Meyer SA, Smith CA, Brindak ME, Fullmer CS, Penniston JT, Kumar R. 1992. Intestinal calcium transport and calcium extrusion processes at the basolateral membrane. J Nutr 122:662-671.

Weekes HC. 1929. On placentation in reptiles. No 1. Proc Linn Soc N S W 54:34-60.

Weekes HC. 1935. A review of placentation among reptiles, with particular regard to the function and evolution of the placenta. Proc Zool Soc Lond 2:625-645.

Wooding FBP, Ramirez-Pinilla MP, Forhead AS. 2010. Functional studies of the placenta of the lizard *Mabuya* sp. (Scincidae) using immunocytochemistry. Placenta 31:675-685.